

Photocatalysis and Self-catalyzed Photobleaching with Covalently-Linked Chromophore-Quencher Conjugates Built Around BOPHY

Dumitru Sirbu, Owen J. Woodford, Andrew C. Benniston and Anthony Harriman*

Molecular Photonics Laboratory, School of Natural and Environmental Science (Chemistry),
Bedson Building, New-castle University, Newcastle upon Tyne, NE1 7RU, United Kingdom.

SUPPORTING INFORMATION

TABLE OF CONTENTS

Compound characterization for the target CSCs	S2
Experimental conditions	S8
Cyclic voltammetry and Frontier Molecular Orbitals	S11
Photobleaching in other solvents	S15
Effect of additives	S16

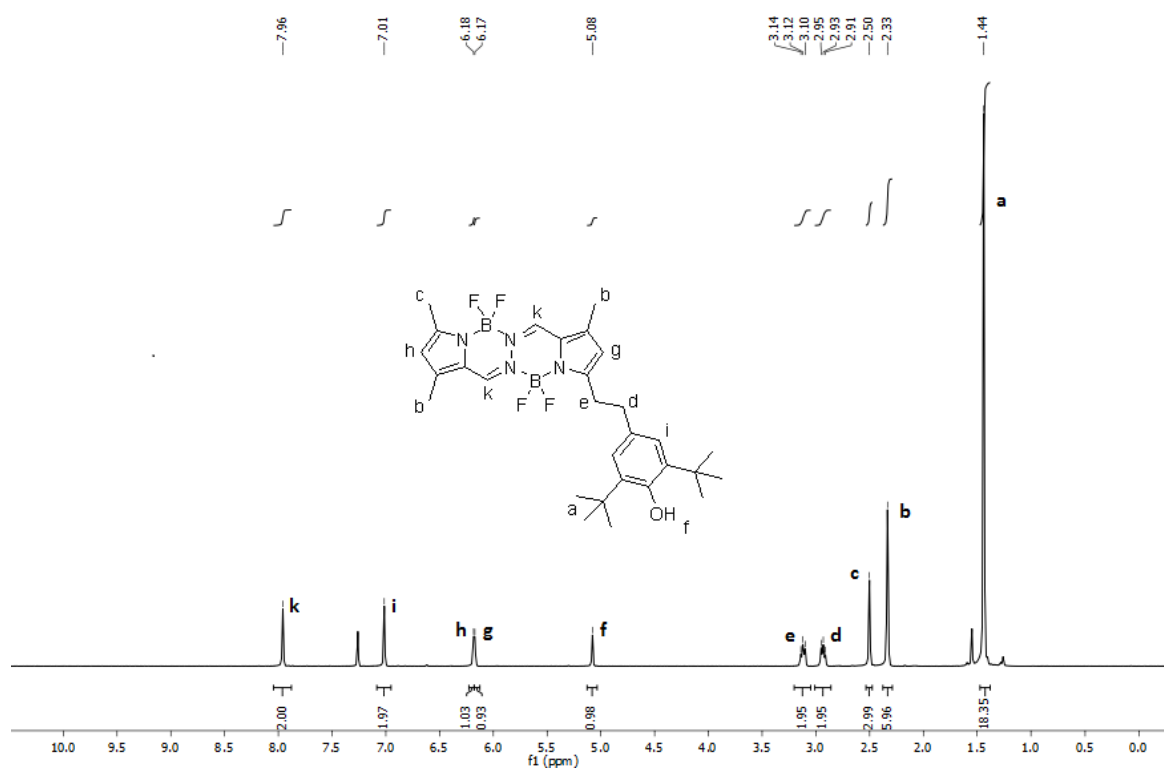


Figure S1. ^1H NMR spectrum for **P1B** in CDCl_3 with peak assignment.

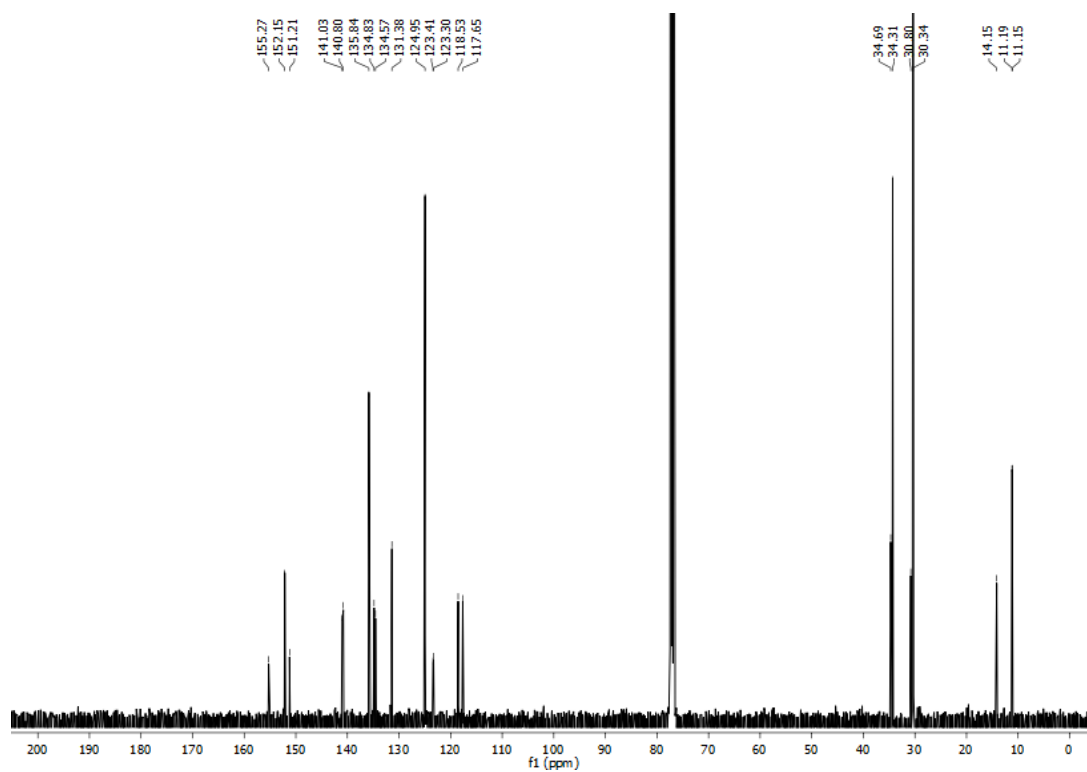


Figure S2. ^{13}C NMR spectrum for **P1B** in CDCl_3 .

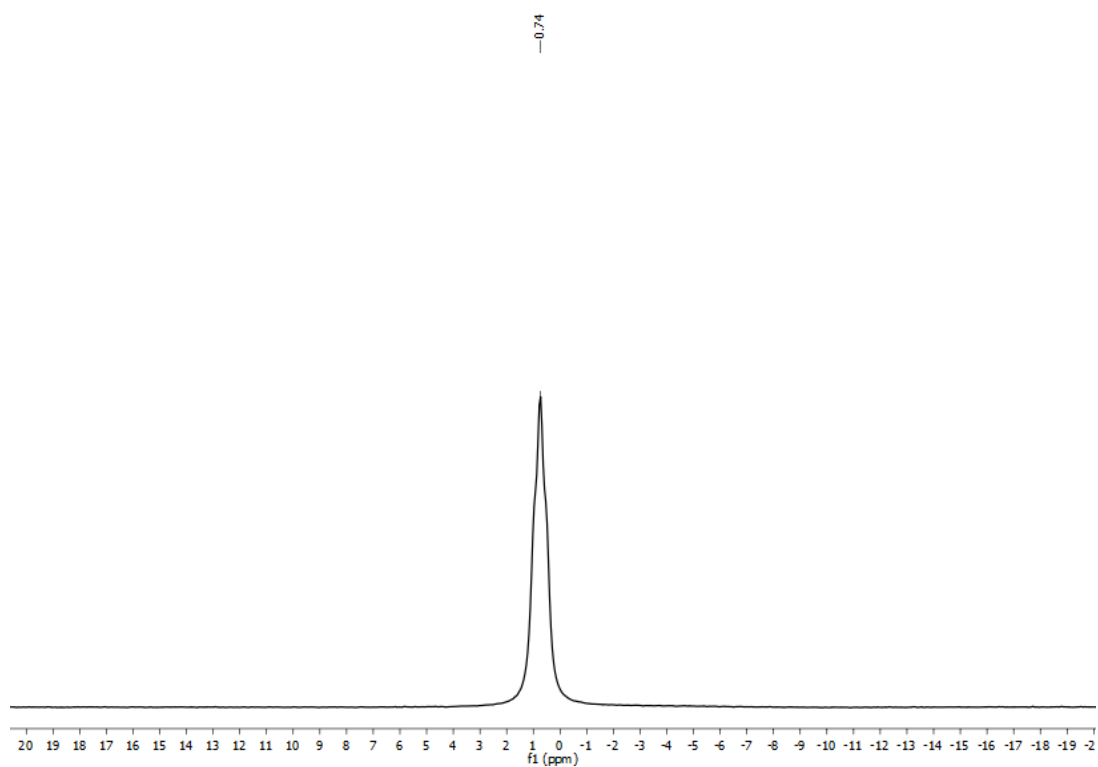


Figure S3. ^{11}B NMR spectrum for **P1B** in CDCl_3 .

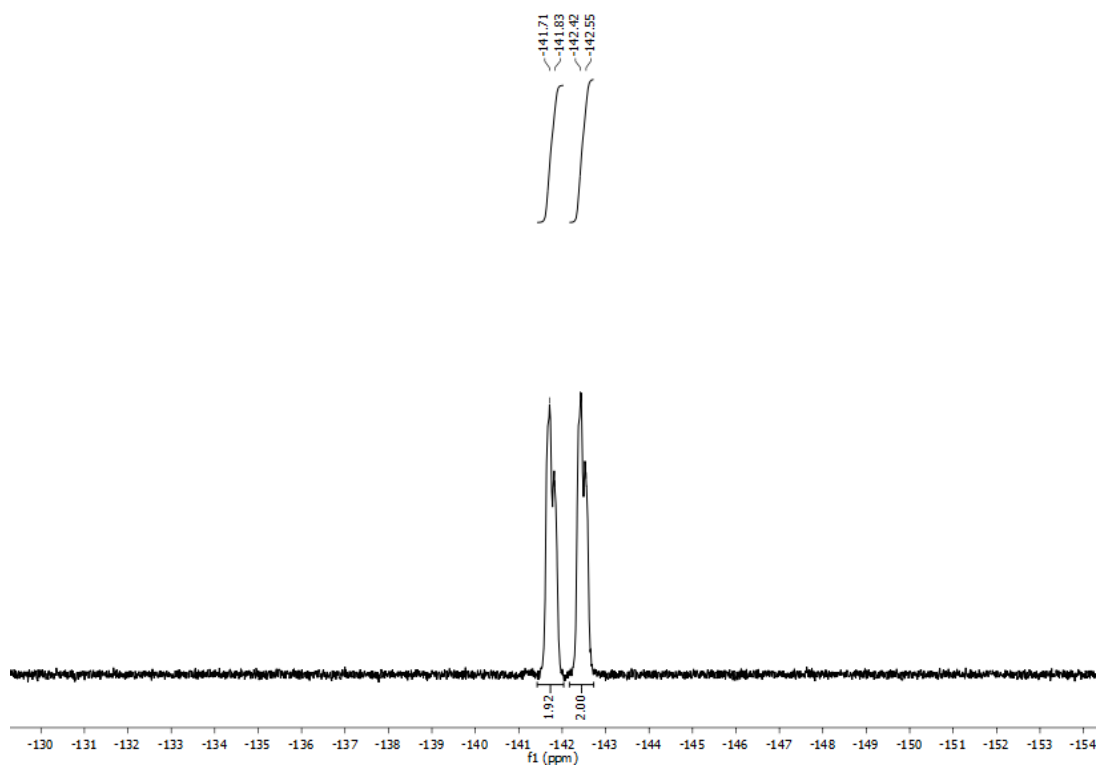


Figure S4. ^{19}F NMR spectrum for **P1B** in CDCl_3 .

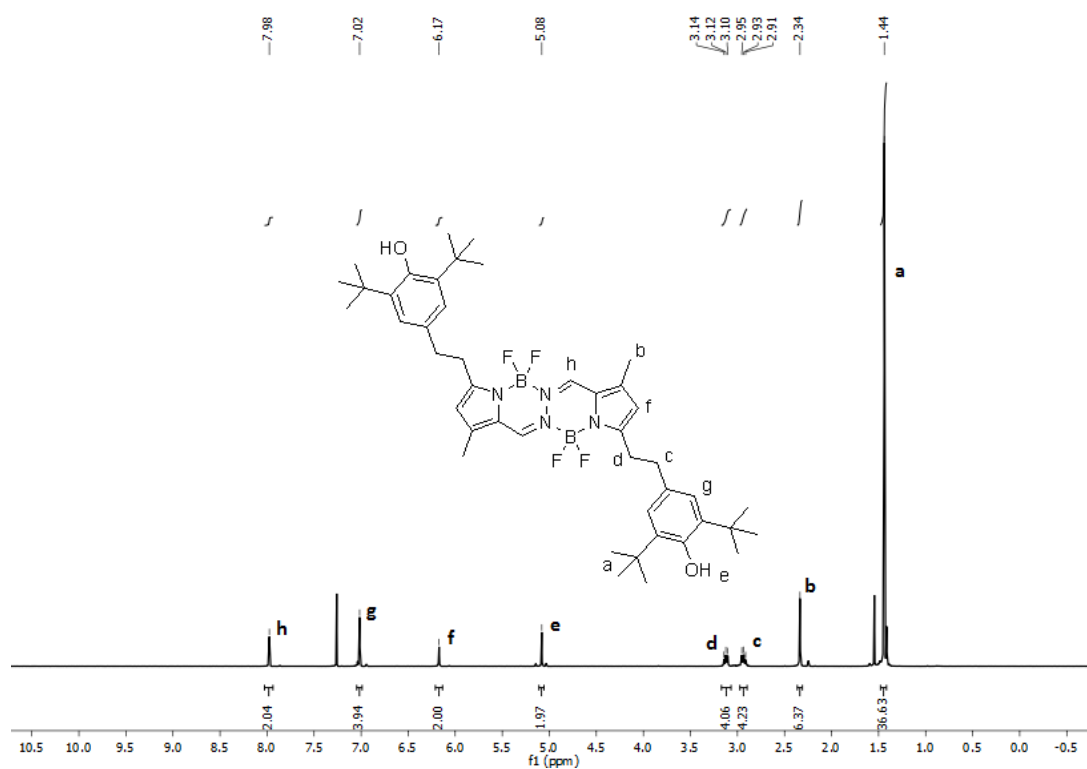


Figure S5. ¹H NMR spectrum for **P2B** in CDCl₃ with peak assignment.

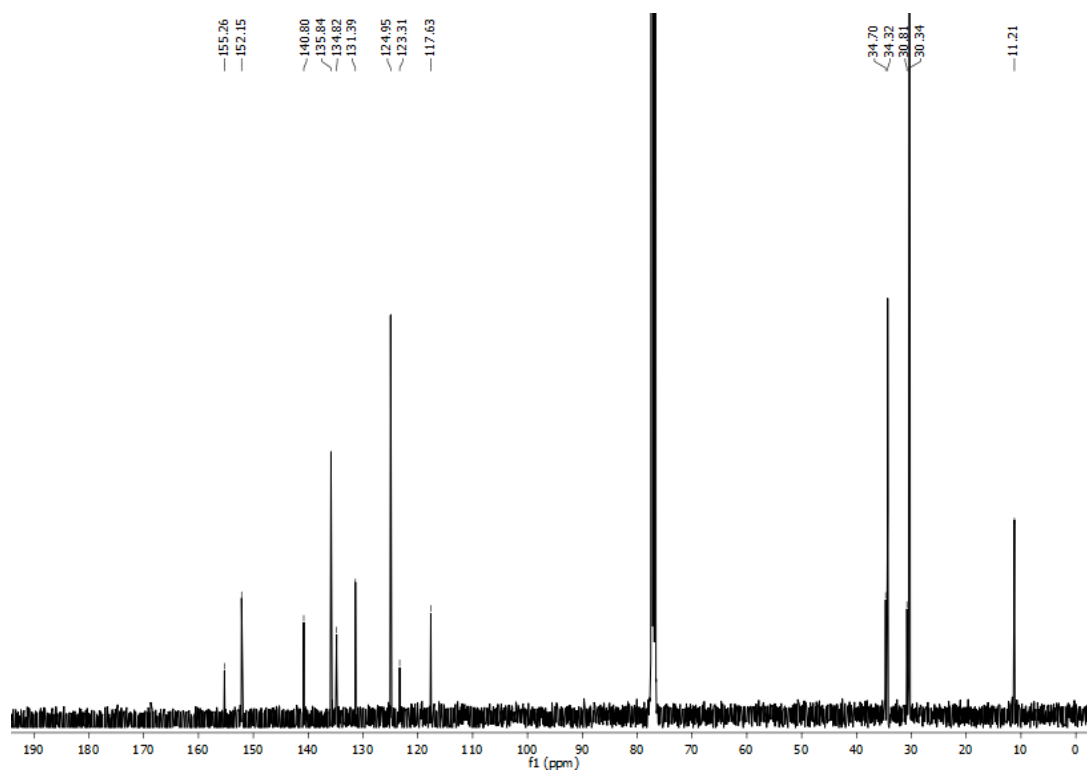


Figure S6. ¹³C NMR spectrum for **P2B** in CDCl₃.

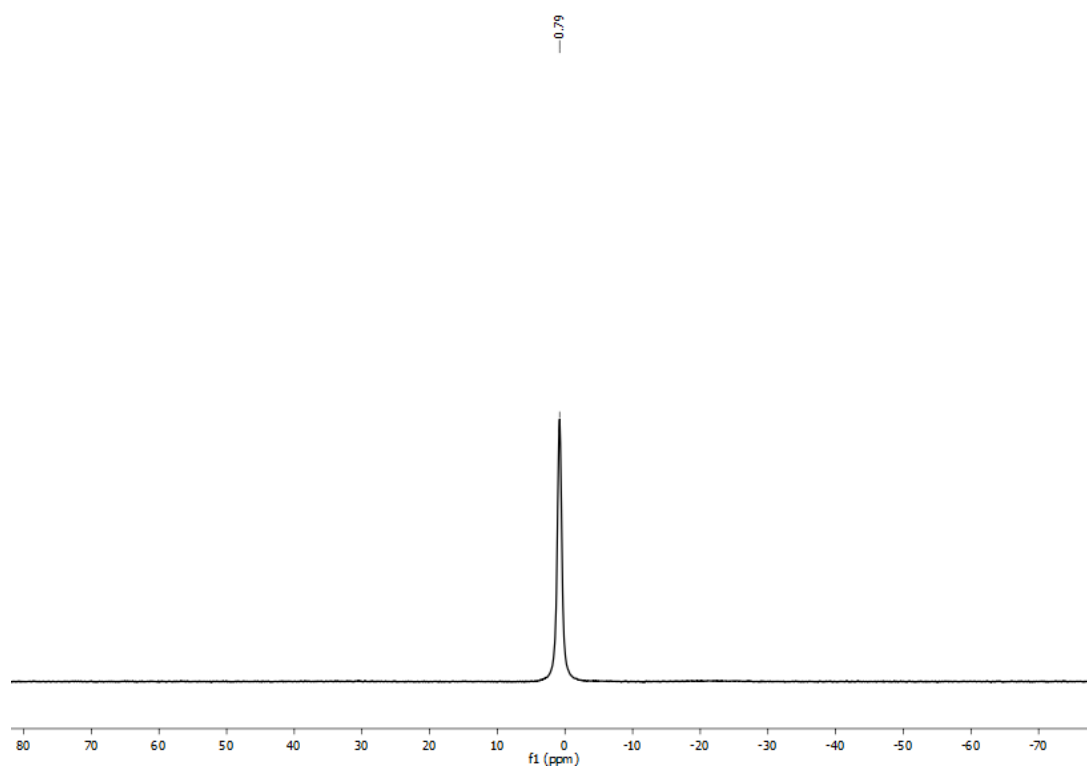


Figure S7. ^{11}B NMR spectrum for **P2B** in CDCl_3 .

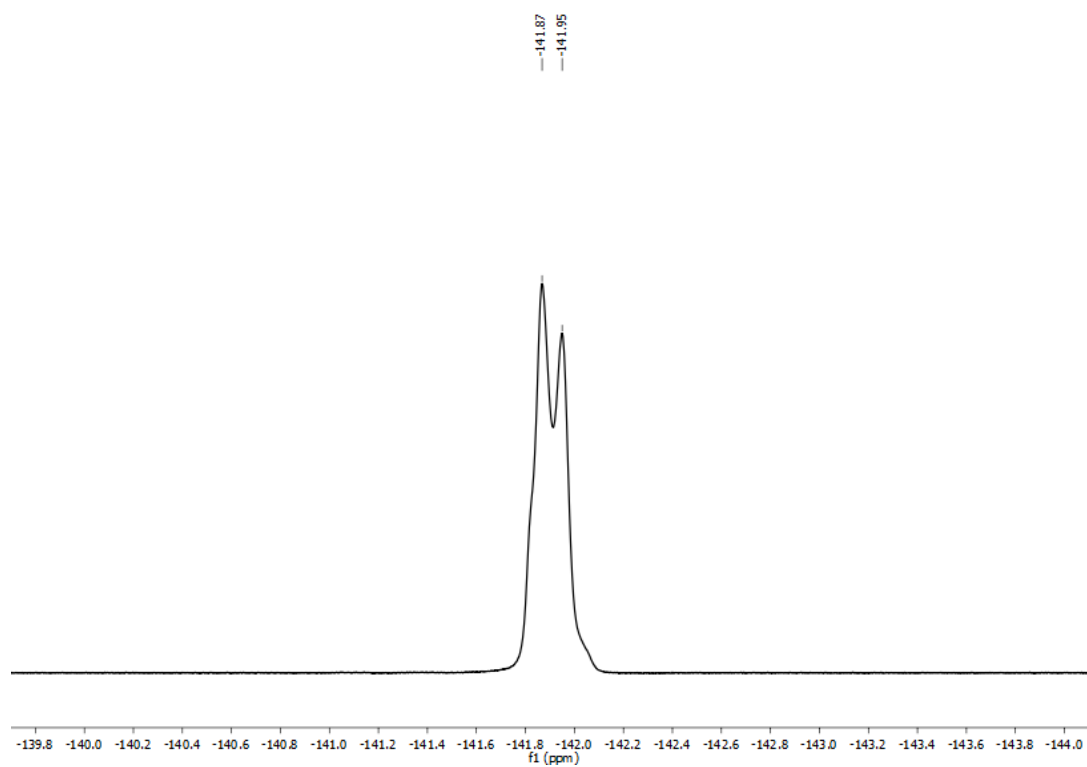


Figure S8. ^{19}F NMR spectrum for **P2B** in CDCl_3 .

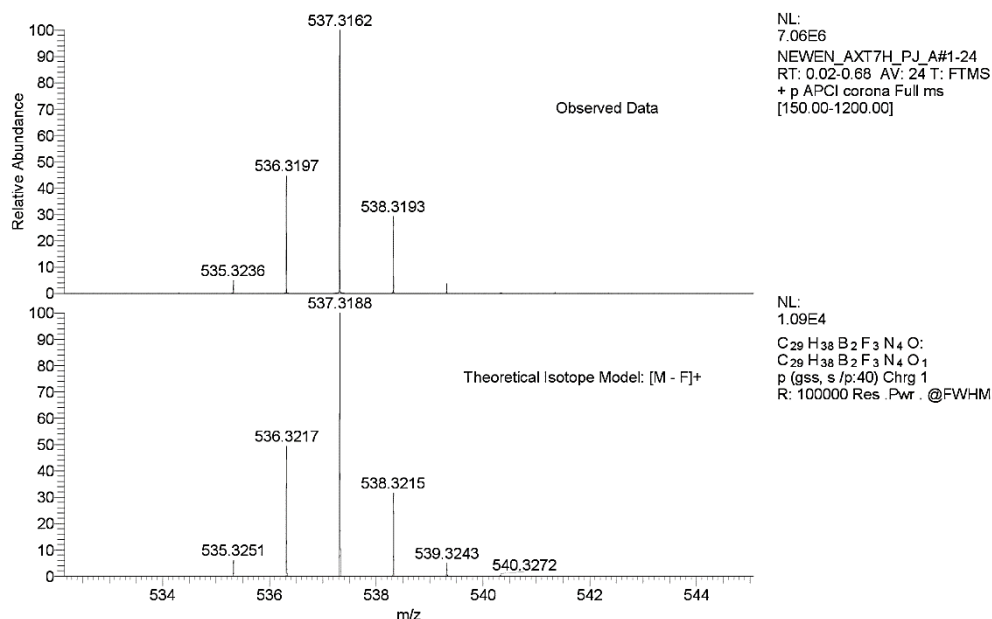


Figure S9. ASAP-APCI FTMS⁺ spectrum for **P1B** showing the [M-F]⁺ cation.

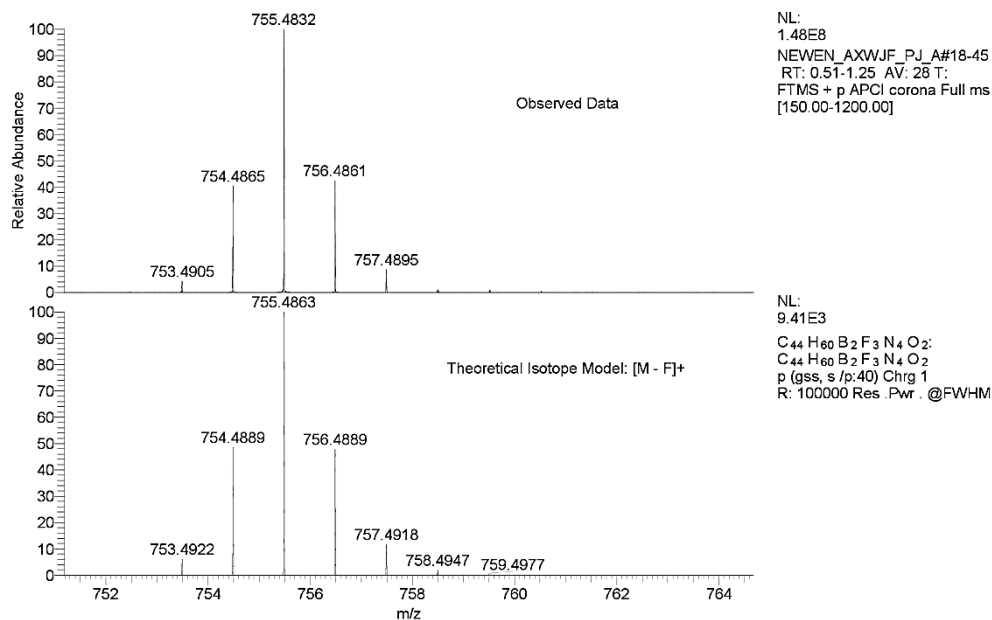


Figure S10. ASAP-APCI FTMS⁺ spectrum for **P2B** showing the [M-F]⁺ cation.

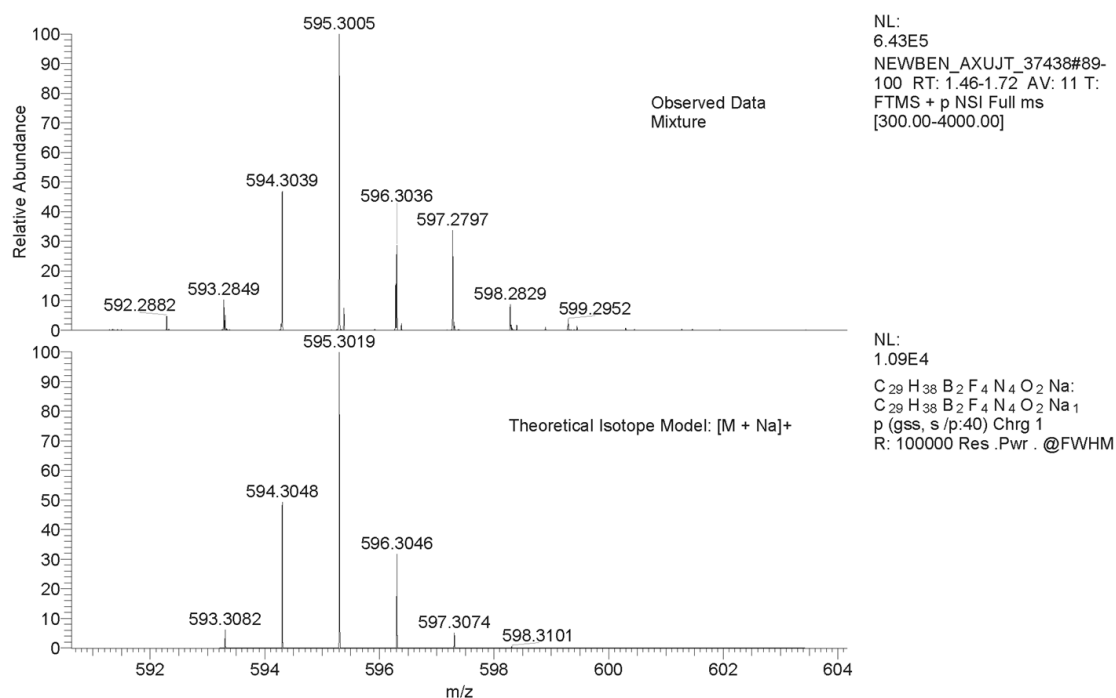


Figure S11. NanoESI FTMS+ spectrum for crude **P1B-OOH** showing the $[M+Na]^+$ cation.

Experimental conditions

Solvents used for the spectroscopic studies were purchased as the highest available grade and were checked for fluorescent impurities before starting the experiment. Additives used in the photobleaching studies were used as received. Absorption spectra were recorded using a Perkin Elmer Lambda 35 spectrophotometer while fluorescence spectra were recorded with a Hitachi F-4500 spectrophotometer. Fluorescence quantum yields were determined for optically dilute solutions, with the absorbance being less than 0.1 at the excitation wavelength. All measurements were repeated four times at slightly different concentrations. Fluorescence lifetimes were measured with a PTI EasyLife LS time-correlated, single photon counting instrument with excitation being provided by a 440-nm pulsed LED (FWHM = 0.35 ns). Data analysis was made by fitting the deconvoluted emission signal to either a single exponential or to the sum of two exponential components as appropriate. The goodness-of-fit was judged by the reduced chi-squared factor and examination of the weighted residuals using standard statistical methods. Fluorescence quantum yield measurements were determined relative to tetra-methyl BOPHY^{S1} in CH₂Cl₂ ($\Phi_F = 0.75$) which in turn was measured relative to Rhodamine 123^{S2} in ethanol solution ($\Phi_F = 0.90$). Corrections were made for changes in refractive index.^{S3}

Transient absorption measurements were made using an Applied Photophysics LKS80 laser flash photolysis system. Excitation was by 4-ns pulses of 20 mJ at 355 nm using the frequency-tripled output from a Nd:YAG laser. The solution was deaerated by purging with N₂ or aerated by standing overnight in the dark. Kinetic measurements were made at fixed wavelength by averaging 50 individual decay records and using different time bases. Differential absorption spectra were compiled point-by-point by averaging five records collected at each wavelength.

Photobleaching of the sample was carried out as described previously.^{S4} The solution was adjusted to have an initial absorbance of unity at the band maximum in a 1-cm pathlength cuvette. The solution was purged with the appropriate gas at atmospheric pressure before being sealed. Illumination was made with a 400W HQI lamp, filtered to remove UV and IR radiation. The sample was positioned 30 cm from the light source and the temperature was checked to ensure no accidental heating of the liquid. The course of reaction was followed by optical spectroscopy. Several runs of the same experiment were made. Quantum yield determinations were made with a 440 nm high-intensity LED as light source. Output is not

monochromatic but restricted to a narrow wavelength distribution. Integration of the output signal with the absorption spectrum of the chromophore allows determination of the total number of absorbed photons. This number changes as bleaching proceeds.

Films were prepared by solution casting. PMMA ($M_w = 120,000$ g/mol) was dissolved in a 3:1 solvent:polymer mass ratio in toluene. After complete dissolution, a fixed aliquot of a concentrated dye stock solution was added with agitation. Solutions were mixed at 40 °C for 2 hours before being poured into 1 mm thick molds. The films were dried at room temperature for 24 hours before being annealed at 80 °C to achieve smooth films having excellent optical quality. Absorption and emission spectra were recorded for different regions of the film to ensure the consistency of the film thickness. Part of the film was covered with protective tape and used as a control by which to follow the course of photobleaching. The film was held in a special holder that allowed accurate positioning in the light beam. for the photobleaching studies.

The same illumination setup was used to polymerize methyl methacrylate. Typically, a small aliquot of P1B was added to the monomer in a test tube so as to give a final concentration of approximately 0.1 mM. The sample was illuminated with white light. The viscosity slowly increased until a solid was formed. During illumination, the colour of the sensitizer faded and, by the time the sample has solidified, the final material was colorless (Figure S12).



Figure S12. Example of the photopolymerized PMMA obtained using P1B as initiator.

Photochemical synthesis of (4-bromophenyl)(pyrrolidin-1-yl)methanone

The solution of 4-bromobenzaldehyde (15 mmol), pyrrolidine (45 mmol) and P2B (0.3 mmol) in 5 mL dioxane under air at 30 °C was illuminated for 24 h with broadband light (30 cm in front of a 400W HQI lamp). The light source was filtered to remove UV irradiation and heat. After photolysis, the reaction mixture was diluted with CH₂Cl₂ and washed with water. The organic layer was dried on MgSO₄, reduced under vacuum and purified by silica gel column chromatography by eluting with hexane / ethyl acetate (3:1) to give the target product as a white solid in 75 % yield. Analysis was made by NMR spectroscopy, with the observed spectrum being in good agreement with the literature.^{S5}

¹H NMR (400 MHz, CDCl₃): δ (ppm) = 7.53 (d, *J* = 8.4 Hz, 2H), 7.40 (d, *J* = 8.4 Hz, 2H), 3.63 (tr, *J* = 6.9 Hz, 2H), 3.41 (tr, *J* = 6.6 Hz, 2H), 2.01 – 1.93 (m, 2H), 1.93 – 1.86 (m, 2H). ¹³C NMR (101 MHz, CDCl₃): δ (ppm) = 168.8, 136.2, 131.6, 129.0, 124.3, 49.8, 46.4, 26.6, 24.6.

Cyclic voltammetry

Cyclic voltammetry was made with a conventional three-electrode set-up using a CH Instruments potentiostat and signal generator. The sample (2 mM) was dissolved in dried CH_2Cl_2 containing tetra-*N*-butylammonium tetrafluoroborate (0.15 M) as background electrolyte. The solution was deaerated with a stream of dried N_2 prior to the experiment. A glassy carbon disc was used as working electrode in conjunction with a Pt wire as counter electrode. The reference electrode was a freshly prepared Ag/Ag^+ electrode isolated from the solution with a porous glass plug. The latter was calibrated by the addition of ferrocene. A range of scan rates was used in each case and the working electrode was polished between successive scans. The reproducibility of peak potentials was better than ± 10 mV. Examples of the cyclic voltammograms recorded for the target compounds are provided as Figures S13 and S14.

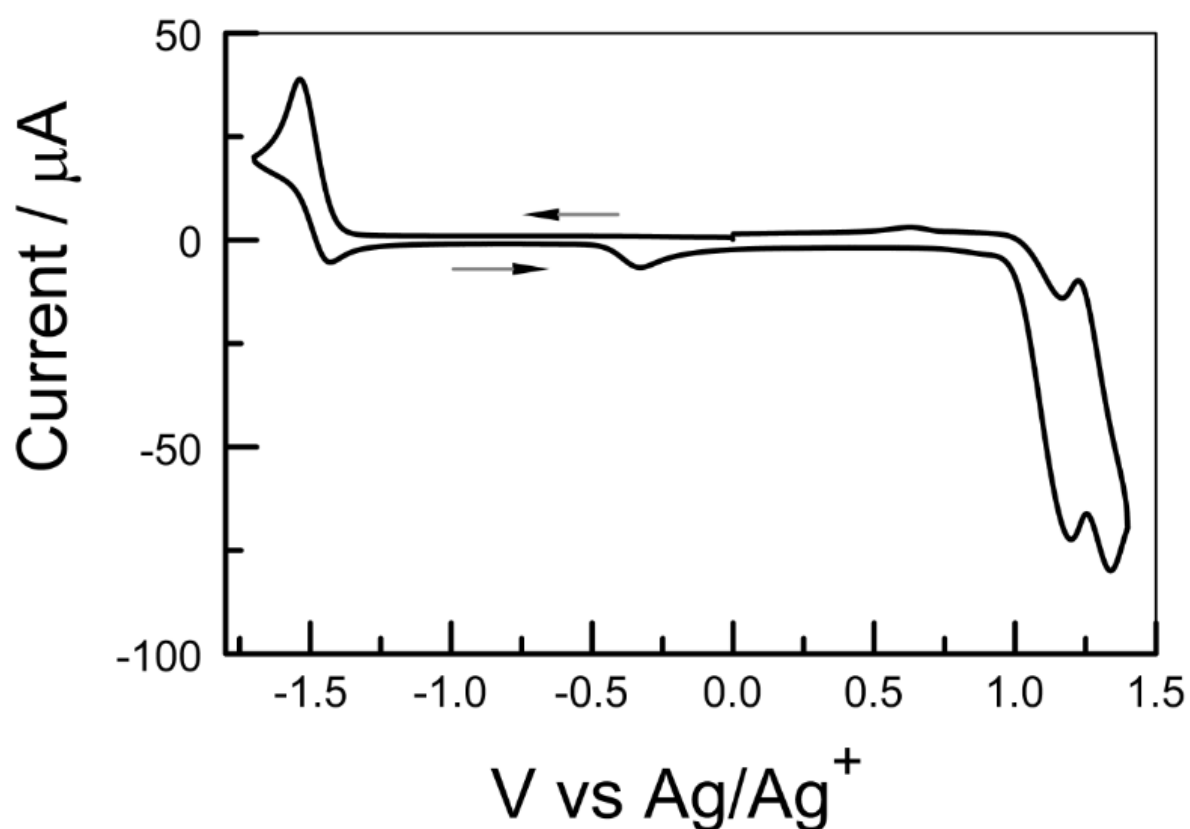


Figure S13. Cyclic voltammogram recorded for P1B in deaerated CH_2Cl_2 containing tetra-*N*-butylammonium tetrafluoroborate (0.15 M).

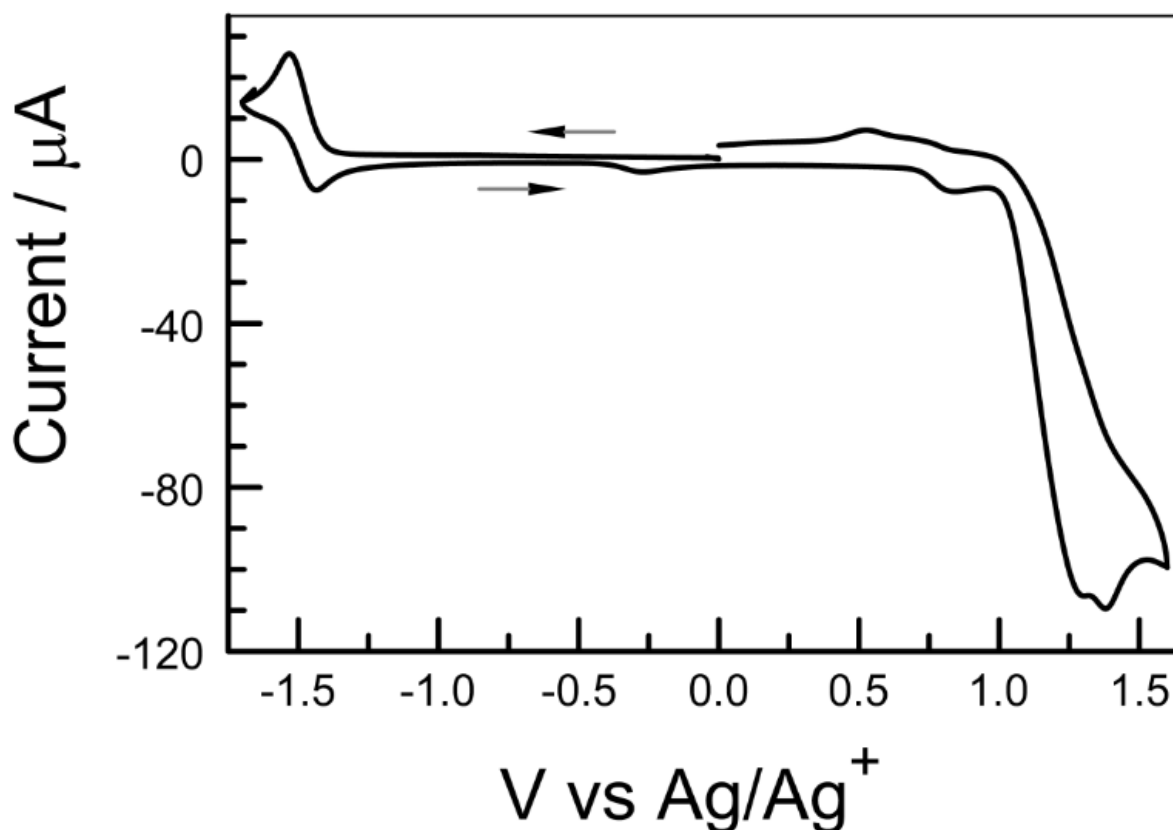


Figure 14. Cyclic voltammogram recorded for P2B in deaerated CH_2Cl_2 containing tetra-*N*-butylammonium tetrafluoroborate (0.15 M).

To help interpret the cyclic voltammograms, a series of calculations was implemented to identify the frontier molecular orbitals. These calculations were made at the DFT level using GAMESS with the PBE0/6-311G(d) force field and with the PCM solvent model (PCM/ CHCl_3). Output is presented below in the form of Kohn-Sham distributions for the relevant MOs. It is seen that the LUMO is centred on the BOPHY nucleus (Figure S15), fully consistent with one-electron reduction occurring at this site to give the BOPHY π -radical anion. The calculation indicate two HOMOs at very close energy which involve electron density being spread over both the BOPHY and the BHT residues. These distributions differ for the two HOMOs. In fact, HOMO has increased involvement of the BHT residue (Figure S16) while HOMO(-1) restores electron density on the BOPHY residue (Figure S17). These latter descriptions are consistent

with the reported ordering of the oxidation steps and in the occurrence of two oxidation processes appearing at similar potentials.

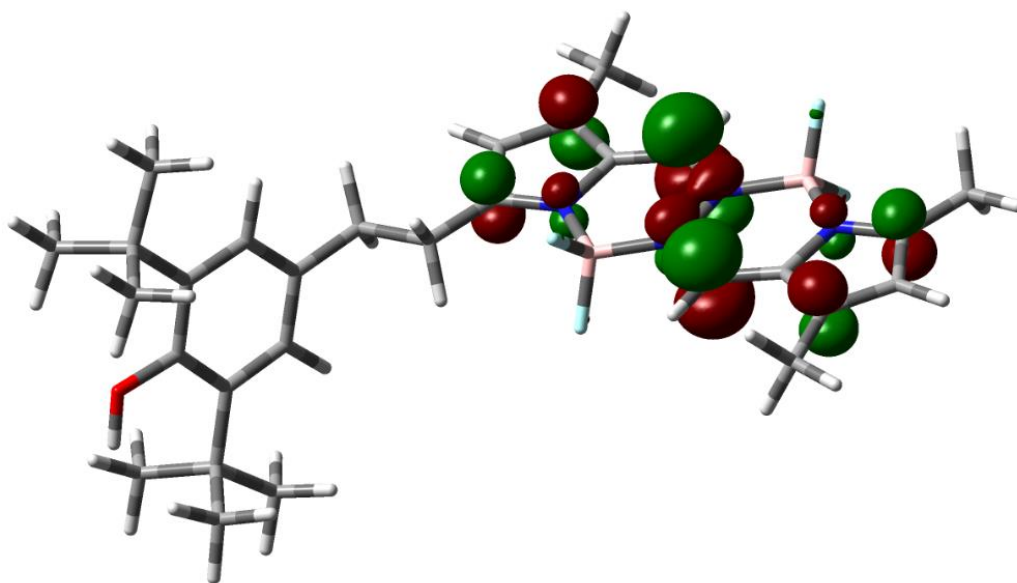


Figure S15. Kohn-Sham distribution for the LUMO calculated for P1B in a reservoir of CHCl_3 molecules.

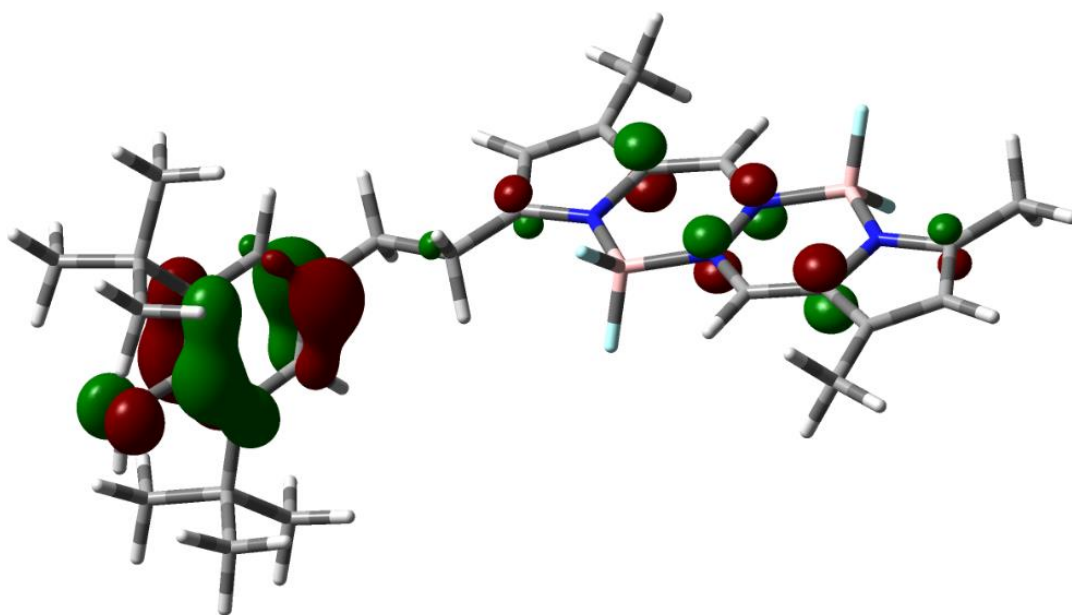


Figure S16. Kohn-Sham distribution for the HOMO calculated for P1B in a reservoir of CHCl_3 molecules.

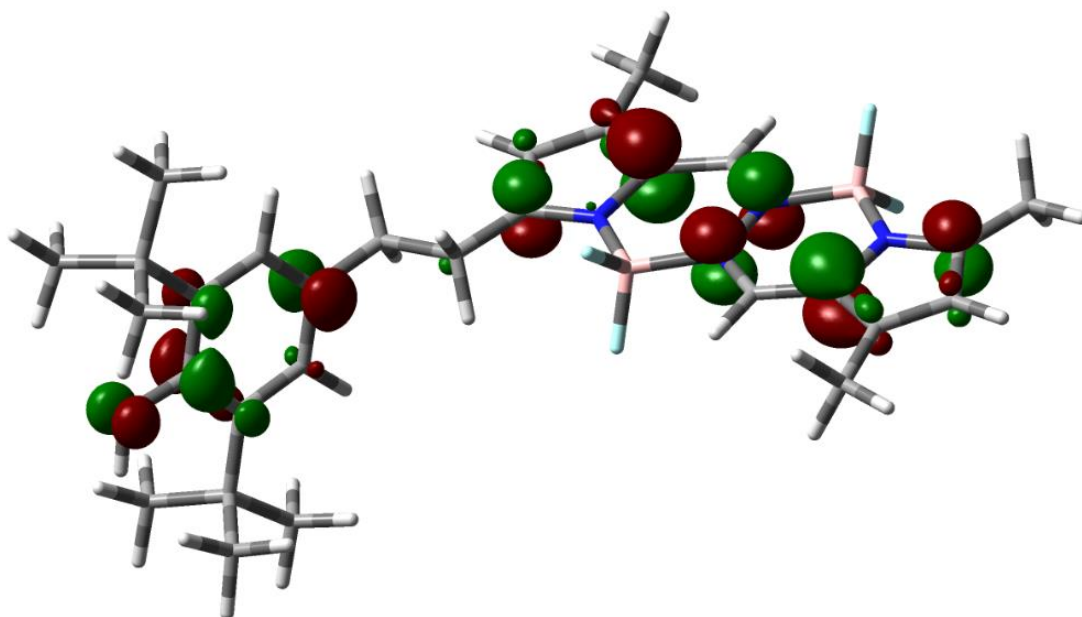


Figure S17. Kohn-Sham distribution for the HOMO(-1) calculated for P1B in a reservoir of CHCl_3 molecules.

REFERENCES

- (S1) I. S. Tamgho, A. Hasheminasab, J. T. Engle, V. N. Nemykin and C. J. Ziegler, A New Highly Fluorescent and Symmetric Pyrrole-BF₂ Chromophore: BOPHY. *J. Am. Chem. Soc.* **2014**, *136*, 5623-5626.
- (S2) T. L. Arbeloa, F. L. Arbeloa, P. H. Bartolome and I. L. Arbeloa, I. L. On the Mechanism of Radiationless Deactivation of Rhodamines. *Chem. Phys.* **1992**, *160*, 123-130.
- (S3) R. S. Knox and H. van Amerongen, Refractive Index Dependence of the Förster Resonance Excitation Transfer Rate. *J. Phys. Chem. B* **2002**, *106*, 5289-5293.
- (S4) O. Woodford, A. Harriman, W. McFarlane and C. Wills, Dramatic Effect of Solvent on the Rate of Photobleaching of Organic Pyrrole-BF₂ (BOPHY) Dyes. *ChemPhotoChem* **2017**, *9*, 3429-3432.
- (S5) (a) K. Ekoue-Kovi and C. Wolf, Metal-free One-pot Oxidative Amination of Aldehydes to Amides. *Org. Lett.*, 2007, *9*, 3429-3432. (b) J. Li, F. Xu, Y. Zhang and Q. Shen, Heterobimetallic Lanthanide/Sodium Phenoxides: Efficient Catalysts for Amidation of Aldehydes with Amines. *J. Org. Chem.*, 2009, *74*, 2575-2577. (c) D. Lednicer, S. C. Lyster and G. W. Duncan, Mammalian Antifertility Agents. IV. Basic 3,4-Dihydronaphthalenes and 1,2,3,4-Tetrahydro-1-naphthols. *J. Med. Chem.* **1967**, *10*, 78-84.

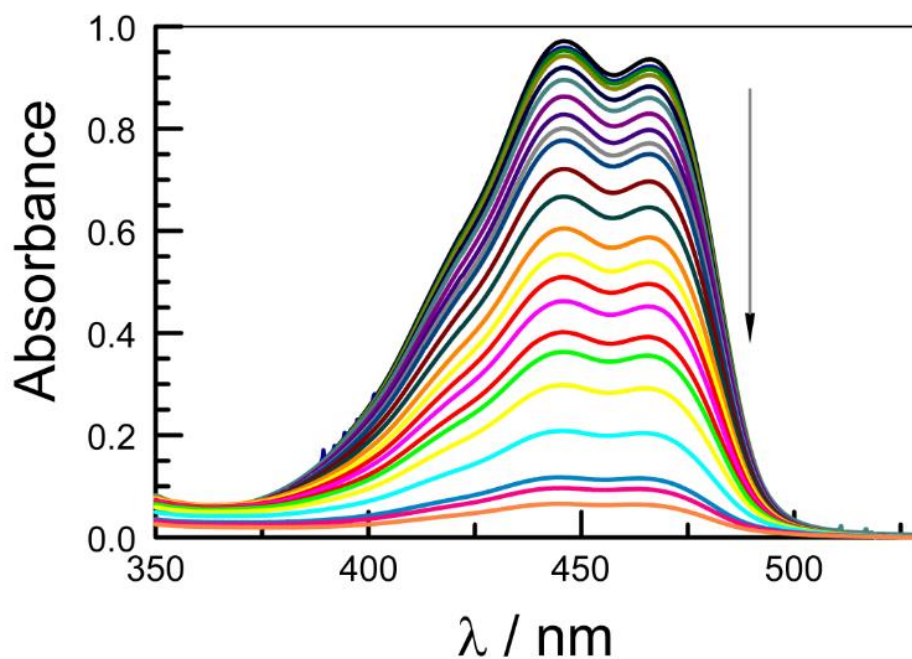


Figure S18. Overlaid absorption spectra showing the course of photobleaching of P2B in air-equilibrated acetone during continuous illumination with white light. Spectra were recorded at regular intervals over a course of 0 to 100 hours.

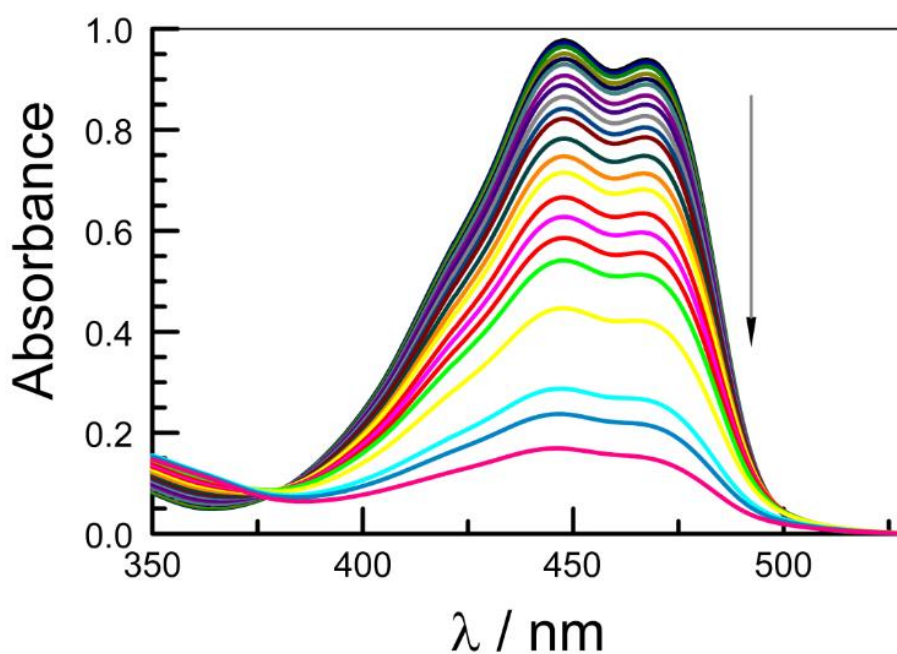


Figure S19. Overlaid absorption spectra showing the course of photobleaching of P2B in air-equilibrated N,N-dimethylformamide during continuous illumination with white light. Spectra were recorded at regular intervals over a course of 0 to 100 hours.

Effects of added quenchers

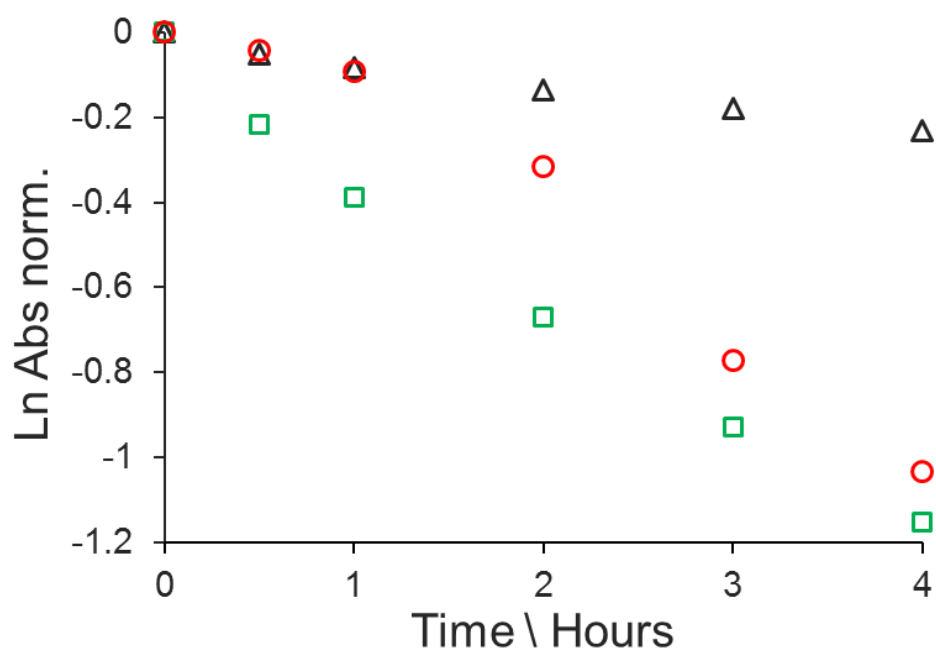


Figure S22. Effect of trapping additives on the photobleaching kinetics determined for P1B in air-equilibrated acetonitrile. The additives are present at 1 mM and refer to Bleaching trapping additives used at 1mM in acetonitrile are DMPO (○) and DABCO (◻). The control experiment without additive is also shown (Δ),

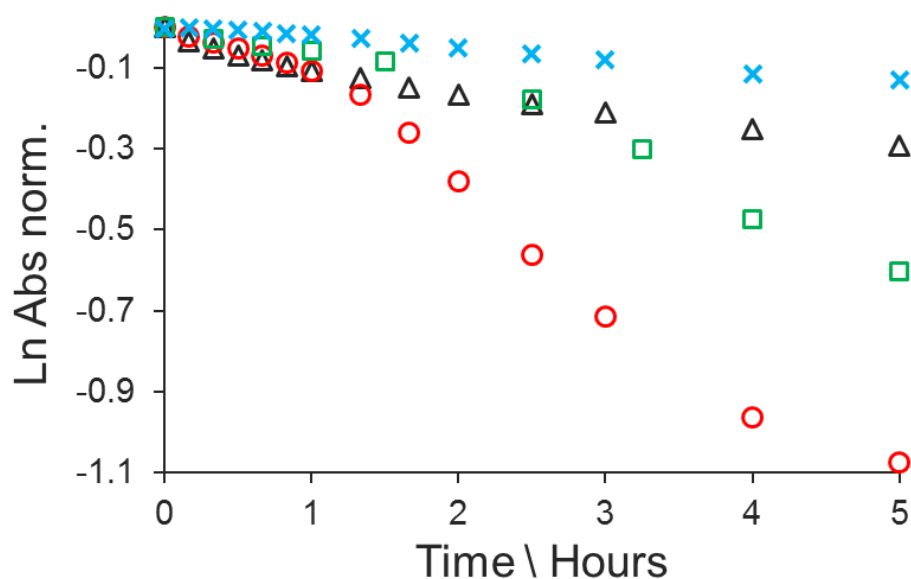


Figure S23. Effect of varying concentration of DMPO on the photobleaching kinetics for P1B in air-equilibrated acetonitrile: control (Δ), 1mM (○), 10mM (◻) and 40mM (×).

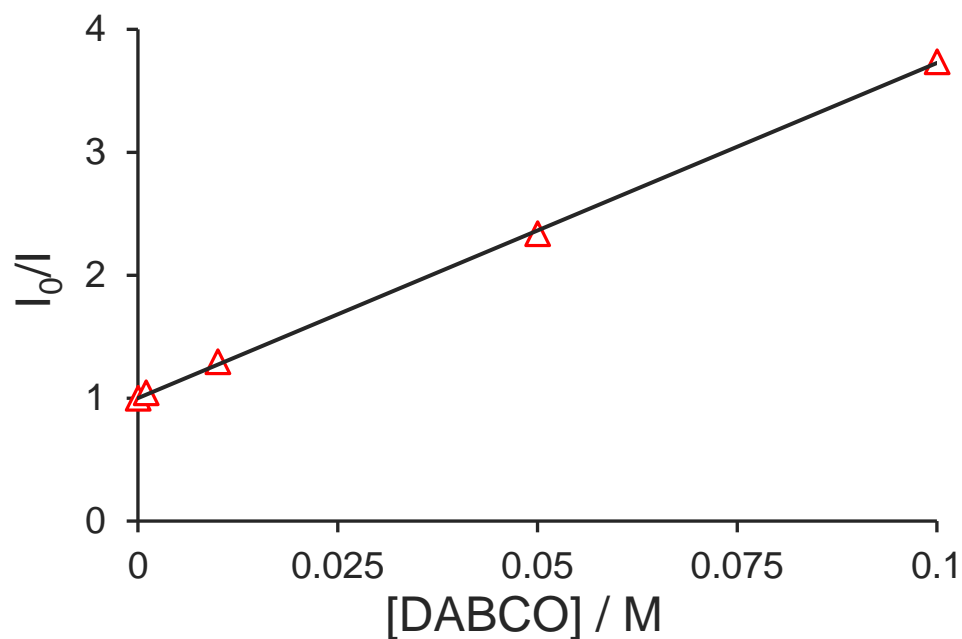


Figure S24. Stern-Volmer plot constructed for the quenching of fluorescence from P1B in acetonitrile at room temperature: $K_{SV} = 27.3 \text{ M}^{-1}$, $k_Q = 2 \times 10^{10} \text{ M}^{-1} \text{ s}^{-1}$ which is the diffusion controlled rate limit in acetonitrile.

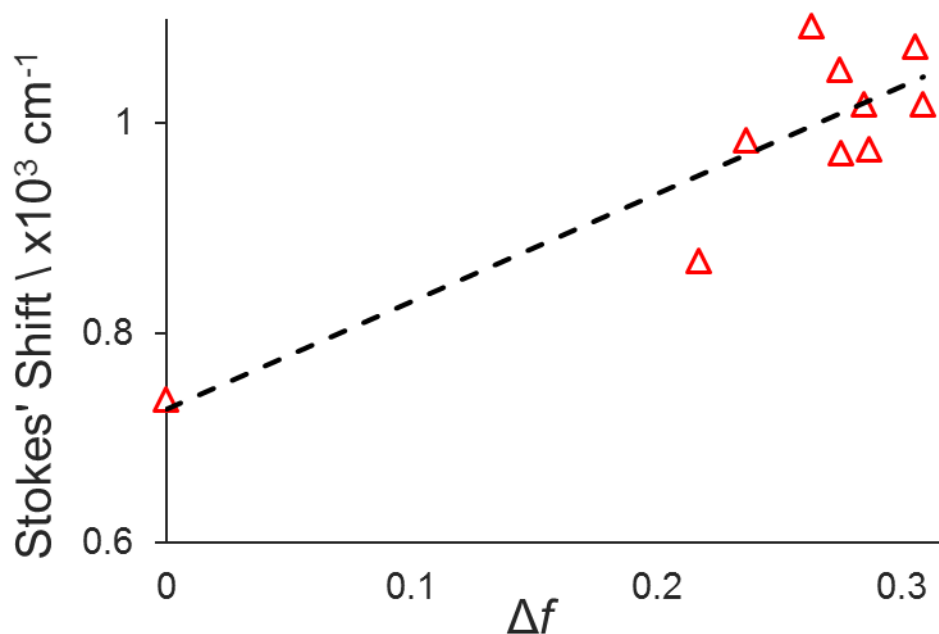


Figure S25. Lippert-Mataga plot for P1B in a small range of solvents as given in Table 1; assuming a molecular radius of 5 \AA the change in dipole moment on excitation is 3.5 D .